Optimal CT Evaluation for Functional Endoscopic Sinus Surgery

Elias R. Melhem, Patrick J. Oliverio, Mark L. Benson, Donald A. Leopold, and S. James Zinreich

PURPOSE: To evaluate the optimal parameters for the CT examination of patients who are having functional endoscopic sinus surgery. **METHODS:** CT scanning was performed on two fresh cadaveric heads in the direct coronal plane, varying the section thickness, intersection gap, scanner gantry angle, and amperage. The nasal cavity and paranasal sinuses were examined independently in a blinded fashion by four staff neuroradiologists and a staff otolaryngologist with special attention to 10 anatomic landmarks within the ostiomeatal unit that are considered important for preoperative planning. A score of 0 (nonvisualization/incomplete visualization) or 1 (clear/complete visualization) was assigned to each of these 10 landmarks. Analysis of variance was used in which reader, subject, and side were simultaneously controlled by "blocking." Multiple comparison methods (ie, Bonferroni) were used to compare the different protocols. **RESULTS:** We found a significant reduction in the delineation, and therefore the perception, of the ostiomeatal unit structures when the section thickness was greater than 5 mm, any intersection gap was used, and the gantry angle was greater than 10° from the plane perpendicular to the hard palate. However, a reduction in the radiation exposure from 200 mA to 80 mA did not affect the display of the anatomic landmarks. **CONCLUSION:** We found the optimal screening CT protocol for the paranasal sinuses to be a section thickness of 3 mm, no intersection gap, and a section angle within 10° from the plane perpendicular to the palate. Also, owing to inherent high contrast between air, soft tissue, and bone in the paranasal sinuses, a reduction in the radiation exposure parameter to 80 mA did not affect image quality.

Index terms: Computed tomography, technique; Paranasal sinuses, computed tomography; Paranasal sinuses, surgery

AJNR Am J Neuroradiol 17:181–188, January 1996

Inflammatory disease of the paranasal sinuses is a common and serious health problem, affecting 30 to 50 million people in the United States alone (1). Functional endoscopic sinus surgery, first introduced in the United States by Kennedy et al (2), has become a popular and effective surgical technique for treating patients with refractory inflammatory sinus disease (incomplete response to medical therapy). The success of functional endoscopic sinus surgery is facilitated by a clear understanding and therefore an accurate display of the anatomy of the nasal cavity and of the paranasal sinuses and their drainage pathways (especially the ostiomeatal unit) in a plane correlating to the surgical orientation.

Direct coronal computed tomography (CT) of sinonasal anatomy displayed by using intermediate window and level settings (window = +1700 Hounsfield units [HU], level = −300 HU) has been established as the imaging technique of choice for examining patients before functional endoscopic sinus surgery because of its simulation of the surgical orientation, adequate depiction of bony and soft-tissue landmarks, and ability to show disease processes (2, 3). In an attempt to decrease cost, examination time, and radiation dose, several variations of CT protocols have been advocated. To date, disagreement continues as to the effect on image quality and definition of anatomic landmarks of variations in section thickness, intersection gap, gantry angle, and exposure parameters in

Received February 16, 1995; accepted after revision July 12.

From the Departments of Radiology and Radiological Science (E.R.M., P.J.O., M.L.B., S.J.Z.) and Otyolaryngology and Head and Neck Surgery (D.A.L.), The Johns Hopkins Medical Institutions, Baltimore, Md.

Address reprint requests to S. James Zinreich, MD, Department of Radiology and Radiological Science, The Johns Hopkins Hospital, 600 N Wolfe St, Baltimore, MD 21287.

AJNR 17:181–188, Jan 1996 0195-6108/96/1701–0181

TABLE 1: Coronal sinus CT imaging protocols

Protocol	mA	Coronal Angle, degrees	Section Thickness, mm	Gap, mm
1	100	0	1.5	0
1A/B	70/40	0	1.5	0
2	100	0	3	0
2A/B	70/40	0	3	0
3	100	0	3	10
3A/B	70/40	0	3	10
4	100	0	5	0
4A/B	70/40	0	5	0
5	100	0	5	10
6	100	0	10	0
6A/B	70/40	0	10	0
7	100	10	3	0
8	100	10	5	0
9	100	20	3	0
10	100	20	5	0
11	100	30	3	0
12	100	30	5	0
13	100	40	3	0
14	100	40	5	0

Note.—In all cases, kV(p) = 120 and time = 2 seconds.

screening patients before functional endoscopic sinus surgery.

Our objective was to identify the optimal coronal CT technique for screening patients before functional endoscopic sinus surgery while keeping in mind patients' safety and comfort as well as maintaining a high-quality operative roadmap for the surgeon.

Methods

CT scans of the nasal cavities and paranasal sinuses of two fresh cadaveric heads were obtained in the prone coronal plane from the anterior wall of the frontal sinus to the clivus using the following scanning parameters: kV(p) = 120, mA = 200, field of view = 14 cm, detail reconstruction algorithm and intermediate window and level settings = +1700 and −300 HU, respectively. The choice of these parameters was based on the preestablished protocols considered optimal for imaging that area (2, 3). At first, the heads were scanned using a section thickness of 1.5 mm and an intersection gap of zero (Table 1, protocol 1). This was used as the standard of reference (Fig 1) given that the smaller structures in the ethmoid sinus are generally less than 5 mm in diameter. Subsequently, different combinations of section thickness and intersection gap (Table 1, protocols 2 to 6) were set, and each head was scanned according to the established protocol.

Subsequently, using the same combinations of section thickness and intersection gap as in protocols 1 to 4 and 6, the two cadaveric heads were rescanned in the coronal plane at 70 mA (Table 1, protocols 1A, 2A, 3A, 4A, and 6A) and 40 mA (Table 1, protocols 1B, 2B, 3B, 4B, and 6B).

Finally, using the same combinations of section thickness and intersection gap as in protocols 2 and 3 only, the paranasal sinuses were rescanned with variations of the coronal plane angle. Scanning was done at 10°, 20°, 30°, and 40° from the plane perpendicular to the hard palate (Fig 2) (Table 1, protocols 7 to 14).

The nasal cavity and paranasal sinuses were examined independently in a blinded fashion by four staff neuroradiologists and a staff otolaryngologist with special attention to 10 anatomic landmarks within the ostiomeatal unit considered to be important for preoperative planning. These include the agar nasi cell, frontal recess, ethmoid bulla, maxillary ostium, infundibulum, uncinate process, middle meatus, basal lamella, and nasolacrimal and olfactory grooves. As a group, the five readers reached a consensus as to the definition of these 10 anatomic structures by reviewing six normal coronal sinus CT examinations from routine clinical service before examining the cadaveric subjects.

A score of 0 (nonvisualization/incomplete visualization) or 1 (clear/complete visualization) was assigned to each of the above landmarks. To be assigned a score of 1, a structure had to be seen in its entirety, with sharp, well-defined margins. Anything less than adherence to this strict criterion resulted in a score of 0. The right and left sides of each cadaveric head were examined independently for each of the above-mentioned protocols (Table 1); a total score from 0 to 10 was assigned (Table 2).

Analysis of variance was used in which reader, subject, and side were simultaneously controlled by "blocking." Multiple comparison methods (ie, Bonferroni) were used to compare the protocols, readers (interobserver variability), sides of the same cadaver, and cadavers.

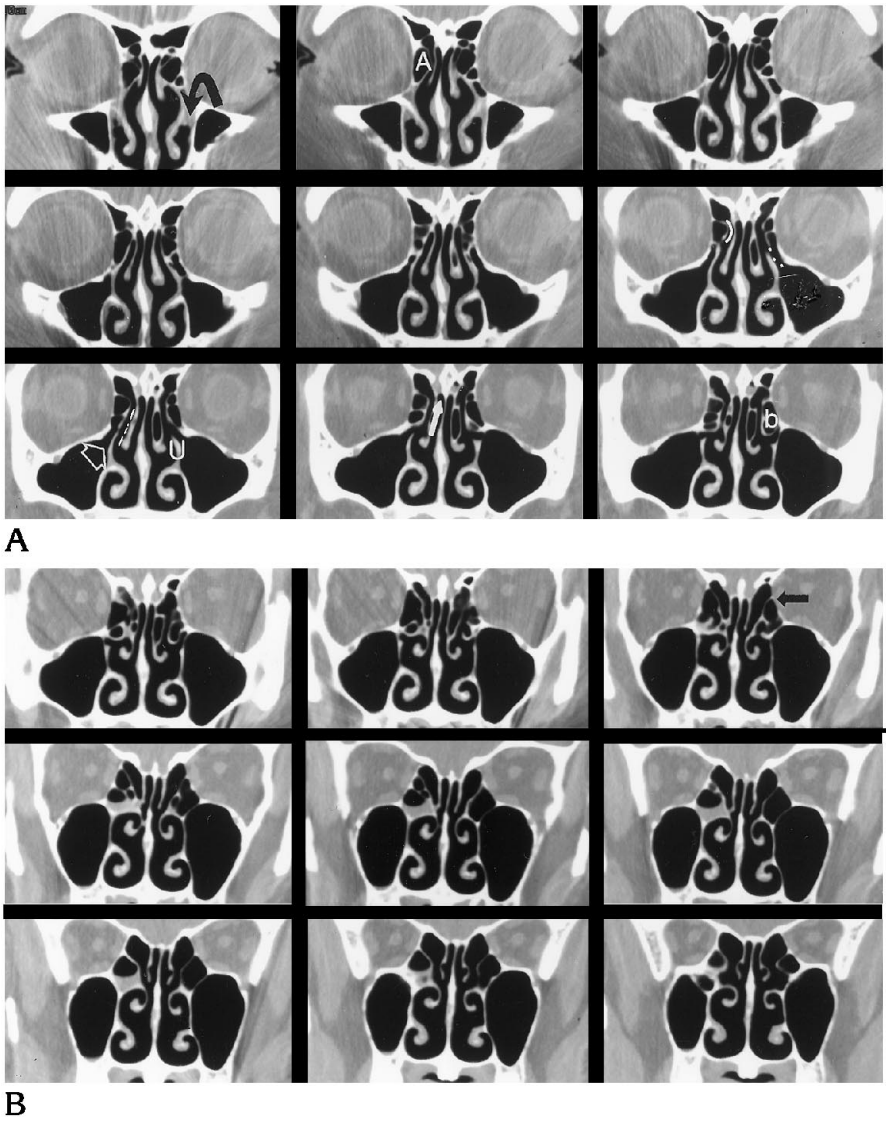

Fig 1. *A* and *B*, Direct coronal CT scans through the paranasal sinuses using a section thickness of 1.5 mm, an intersection gap of zero, a gantry angle of zero (perpendicular to the palate), and 200 mA (standard of reference). Clearly seen are the infundibulum (*dotted line*), frontal recess (*curved line*), middle meatus (*dashed line*), agar nasi cell (*A*), ethmoid bulla (*b*), maxillary ostium (*open arrow*), uncinate process (*U*), basal lamella (*straight black arrow*), nasolacrimal duct (*curved black arrow*), and olfactory groove (*straight white arrow*).

Results

The Bonferroni *t*-test analysis performed on the mean total scores of the different protocols with simultaneous control of reader, subject (cadaveric heads), and side showed that (*a*) only protocols 2 (Fig 3) and 7 were within 2 times the standard error of the mean from the standard of reference (protocol 1); (*b*) the mean scores of protocols 5, 6, 13, and 14 were more than 5 times the standard error of the mean; and (*c*) protocols 1A/B, 2A/B, 3A/B, 4A/B, and 6A/B had identical mean scores as their corresponding protocols. The implications include a statistically significant decrease in the definition of the anatomic landmarks contributing to the ostiomeatal unit and distortion of the surgical orientation with a section thicknesses of 5 mm or greater and gantry angles of 20° or greater and a marked deterioration of anatomic detail with section thicknesses approaching 10 mm, intersection gaps of 10 mm, or gantry angles approaching 40° (Figs 4–6). However, there was no effect on the anatomic detail with the decrease in exposure parameters (reduction from 200 mA to 80 mA) (Fig 7).

Simultaneous control of protocol, subject, and side revealed a statistically significant interobserver variability ($P < .05$) despite strict and concise criteria defining the location and clarity of the different anatomic landmarks that were agreed upon by the observers before the start of the study.

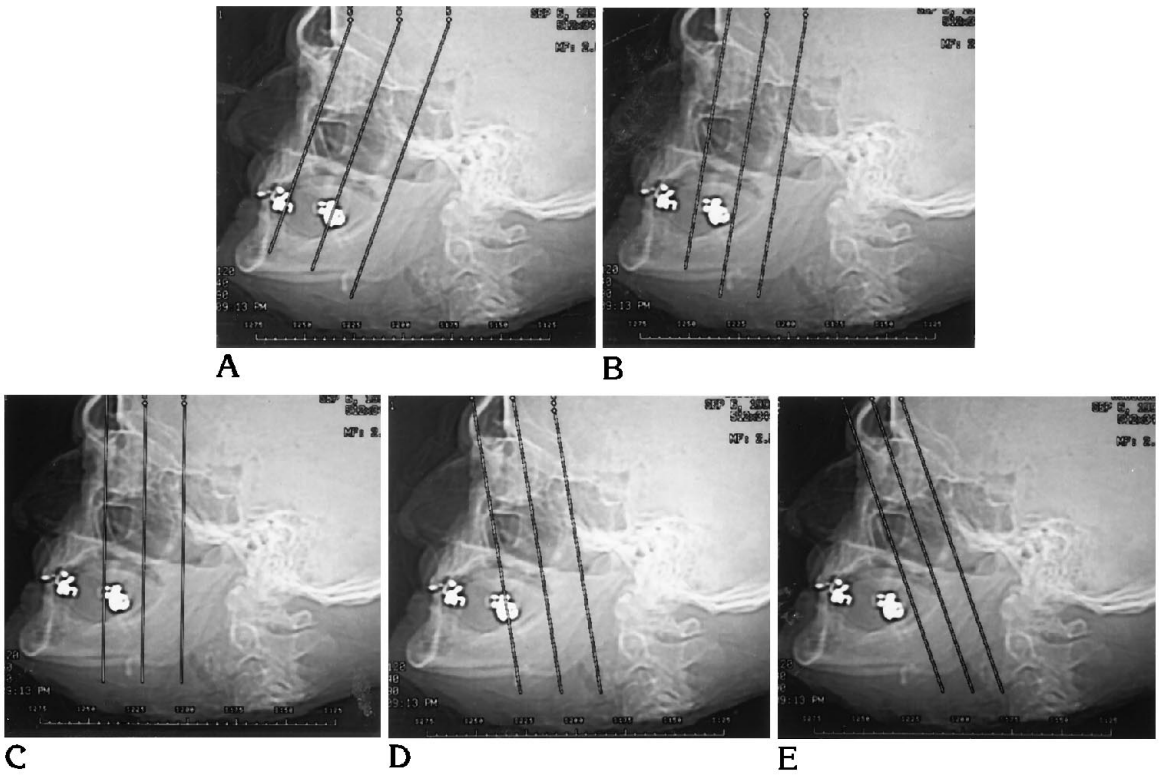

Fig 2. *A–E*, CT topograms of the paranasal sinuses of one of the cadaveric subjects show the different gantry angles used: 0° (from the plane perpendicular to the palate) (*A*), 10° (*B*), 20° (*C*), 30° (*D*), and 40° (*E*).

TABLE 2: Aggregate scores for the ostiomeatal unit for each protocol

	Reader 1				Reader 2				Reader 3				Reader 4				Reader 5			
Subject	1		2		1		2		1		2		1		2		1		2	
Protocol	R	L	R	L	R	L	R	L	R	L	R	L	R	L	R	L	R	L	R	L
1	10	10	9	9	10	10	10	10	10	10	9	9	10	10	10	10	10	10	10	10
2	9	9	4	7	10	10	9	9	10	10	6	7	10	10	8	9	9	9	10	7
3	5	5	4	8	7	7	5	4	7	5	4	4	8	6	6	9	4	4	6	1
4	7	7	3	5	8	8	5	8	8	7	3	5	8	7	7	6	6	5	2	3
5	4	4	1	1	3	3	4	4	4	4	1	2	5	4	5	4	4	3	1	0
6	3	3	1	2	5	5	5	6	3	4	2	3	5	4	4	5	3	1	2	1
7	9	9	6	8	8	8	8	8	9	9	4	7	10	10	6	7	9	8	10	7
8	7	6	4	6	7	7	7	7	6	6	5	7	9	7	4	7	8	5	7	2
9	6	7	6	5	9	9	8	10	7	8	4	6	9	9	7	8	9	5	8	4
10	8	7	5	5	8	7	8	7	8	7	4	5	8	6	4	6	8	4	6	4
11	7	6	4	7	8	8	7	8	7	7	4	7	7	7	3	6	6	4	4	4
12	3	3	5	8	5	5	7	8	6	5	4	6	6	6	3	5	4	3	3	5
13	3	3	4	5	6	6	6	6	4	4	4	5	6	6	4	5	4	3	4	5
14	5	3	2	3	4	4	6	7	4	3	4	3	5	3	1	1	3	2	1	1

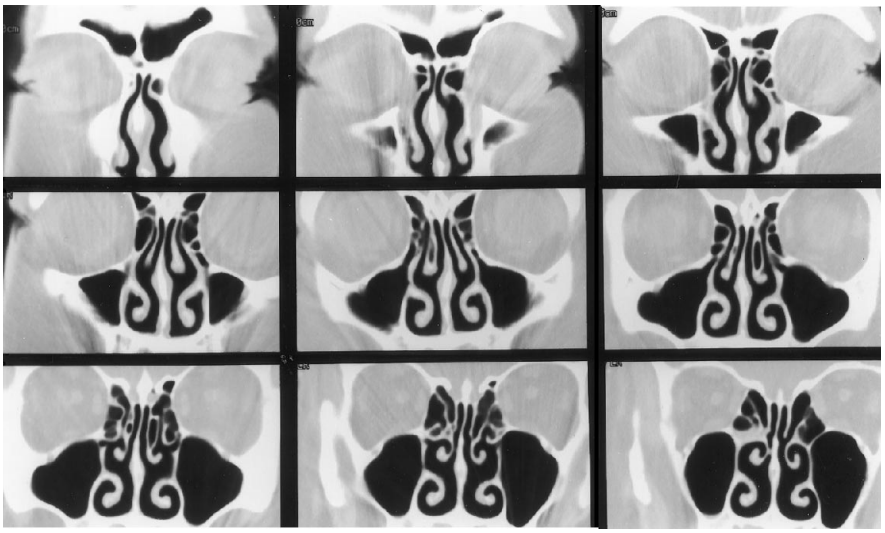

Fig 3. Direct coronal CT scans through the paranasal sinuses using a section thickness of 3 mm, an intersection gap of zero, a gantry angle of zero (perpendicular to the palate), and 200 mA. These parameters produced good definition of all the selected anatomic landmarks, approaching the standard of reference.

A statistically significant difference ($P < .05$) was detected between the mean scores assigned to the images obtained from the two cadaveric heads while controlling for different protocols, readers, and sides. This implies that the effect of normal anatomic variability commonly seen in imaging of the sinonasal structures is represented to a certain extent in our limited sample size.

Discussion

Modern theories regarding the pathogenesis of paranasal sinusitis implicate obstruction of the mucociliary clearance channels ventilating the paranasal sinuses (4–6). Functional endoscopic sinus surgery has largely replaced traditional surgical techniques for reestablishing the normal drainage patterns of the obstructed

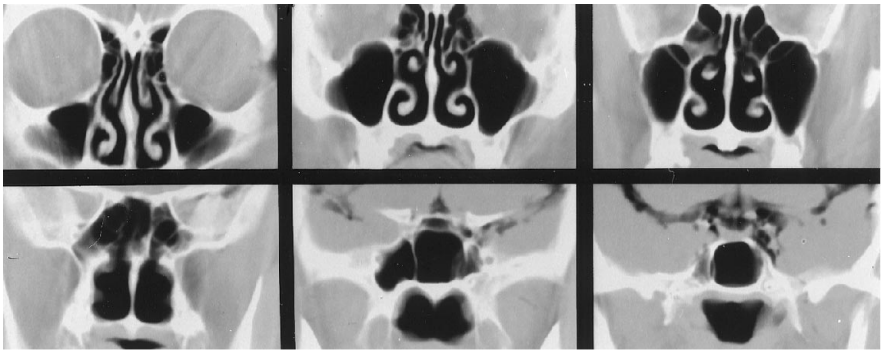

Fig 4. Direct coronal CT scans through the paranasal sinuses using a section thickness of 10 mm, an intersection gap of zero, a gantry angle of zero (perpendicular to the palate), and 200 mA. Use of these parameters resulted in poor definition of the selected anatomic landmarks.

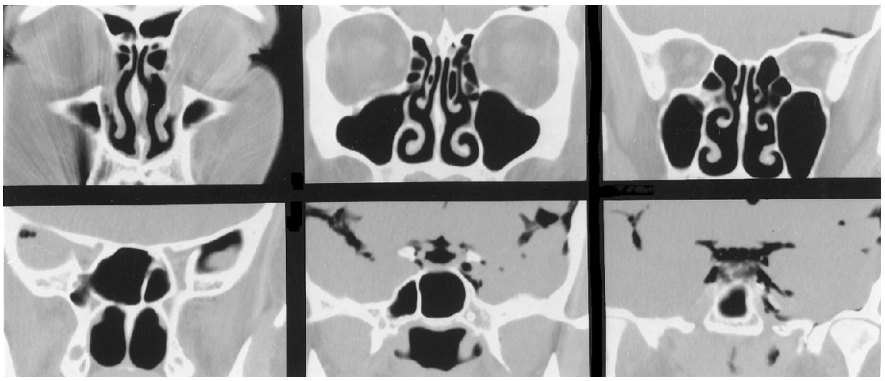

Fig 5. Direct coronal CT scans through the paranasal sinuses using a section thickness of 3 mm, an intersection gap of 10 mm, a gantry angle of zero (perpendicular to the palate), and 200 mA. These parameters produced particularly poor definition of the ethmoid bulla, infundibulum, and uncinate bilaterally.

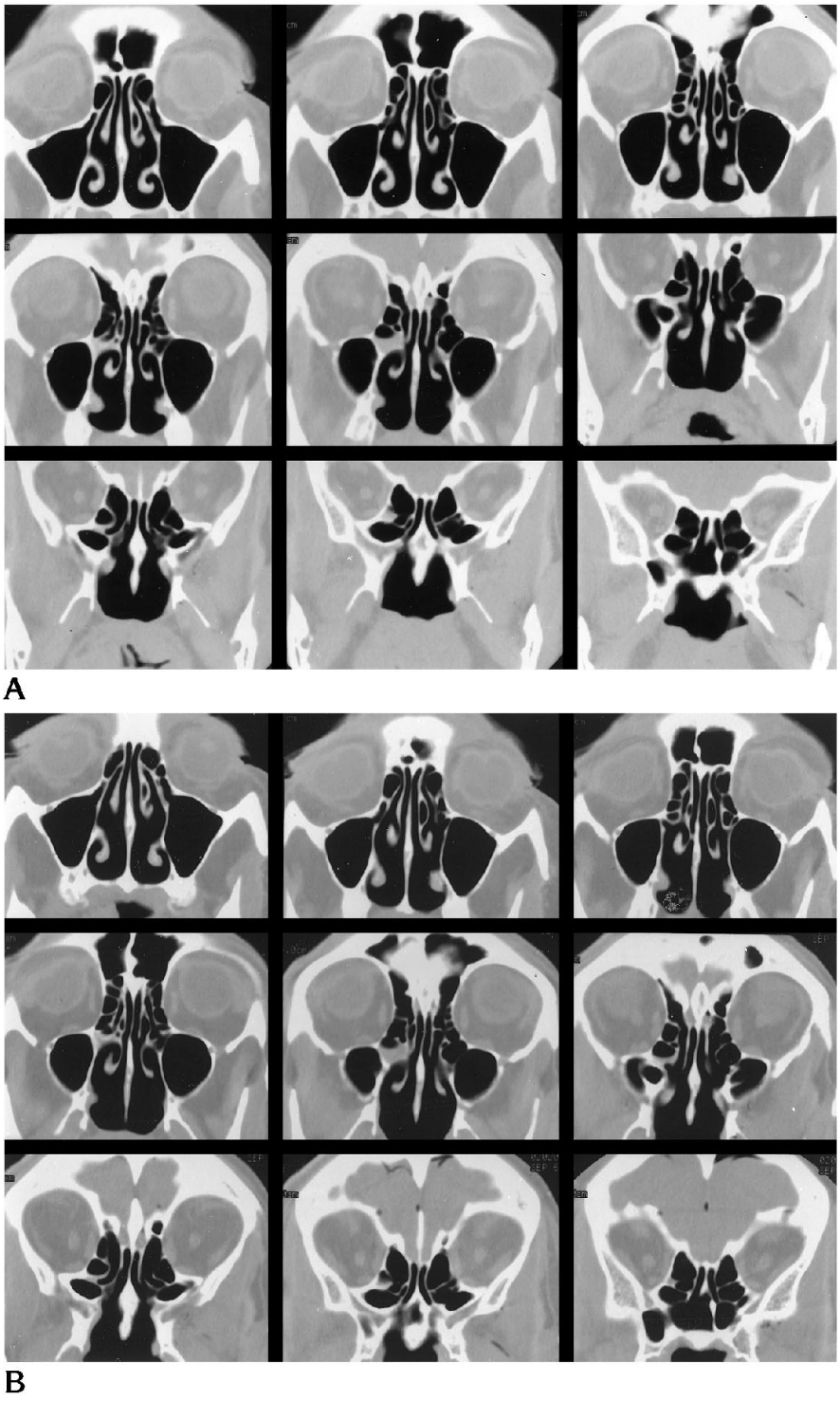

Fig 6. *A* and *B*, Direct coronal CT scans through the paranasal sinuses using a section thickness of 3 mm, an intersection gap of zero, a gantry angle of 30° (*A*) and 40° (*B*) from the plane perpendicular to the palate, and 200 mA. These parameters resulted in poor definition of the selected anatomic landmarks and their surgical orientation.

pathways in patients with refractory chronic sinusitis (7).

Coronal CT of the sinonasal complex has been shown to be the best imaging technique for simulating the endoscopic spatial orientation and for providing an operative roadmap, thus improving the surgeon's perception in an attempt to reduce complications of surgery (eg, diplopia, blindness, leakage of cerebrospinal fluid, and intracranial hemorrhage) (8).

The optimal CT technique for imaging the sinonasal complex is still a matter of debate.

Fig 7. *A–C*, Direct coronal CT scans through the paranasal sinuses using a section thickness of 3 mm, an intersection gap of zero, a gantry angle of zero (perpendicular to the palate), and 200 mA (*A*), 140 mA (*B*), and 80 mA (*C*). These parameters resulted in no loss of definition of the selected anatomic landmarks despite a drop in the exposure parameters by a factor of 2.5.

Several imaging protocols have been proposed, including the "CT mini-series" (9), the "modified CT mini-series" (10), and the "screening coronal section CT scan" (11), but they may not meet the requirements for screening patients before functional endoscopic sinus surgery. Other investigators have suggested that variations in the CT gantry angle up to 40° from the plane perpendicular to the palate and a decrease in the exposure parameters (amperage) have no effect on visualization of the anatomic landmarks and on the surgical orientation (12, 13).

A limited CT examination of the sinuses may be useful for detecting inflammatory disease; however, this type of examination makes it difficult to reproduce the exact positioning on subsequent scans, which decreases the accuracy of follow-up examinations. Further, a limited scan does not provide a complete surgical roadmap. Patients screened with these studies who go on to have functional endoscopic sinus surgery will require an additional study before surgery.

In our study, we addressed the above issues in a prospective manner while keeping in mind that the role of CT in sinus disease is to display the regional anatomy and to identify the anatomic factors that may be the cause of recurrent chronic inflammatory disease. The objective was to provide the surgeon with preoperative and intraoperative roadmaps of the anatomy, while minimizing cost, scanning time, and the patient's exposure to radiation.

Concerning radiation exposure, the radiation dose equivalent is dependent on the kilovoltage and the amperage. For a given kilovoltage, radiation dose equivalent will vary linearly with the amperage. At 125 kV(p), the radiation dose equivalent for a CT section is approximately 1.1 to 1.2 cSv/100 mA. The actual dose will vary slightly from machine to machine. Table 3 shows that the radiation dose equivalent for a CT section can be considerably reduced by using low amperage. In addition, the reduction of exposure parameters (amperage) by a factor of 2.5 did not affect image quality and diagnostic utility, because the inherent high contrast between bone and air in the sinonasal complex is more heavily reliant on spatial resolution (pixel size and section thickness) than on noise.

Our analysis reconfirmed that section thickness and intersection gap significantly affect the ability to fulfill the goals stated above (2, 3, 12). However, in contrast to the findings of Babbel et al (12), we found that the scanning angle has a significant effect not only on the delineation of the ostiomeatal unit but also on preoperative and intraoperative anatomic orientation.

The rotation of the gantry used in this study brings the image orientation into a plane perpendicular to the predicted pathway of the endoscope. An angled endoscope renders a view corresponding to an image plane perpendicular to the hard palate. The radiographic representation of the intranasal structures will not correspond to the endoscopic view if there is excessive angulation in either direction. In daily practice, when performing coronal examinations with the patient in the prone position, the

TABLE 3: Relative radiation dose for sinus CT

mA	Radiation Dose Equivalent, cSv*
450	4.95 – 5.40
240	2.64 – 2.88
160	1.76 – 1.92
80	0.88 – 0.96

* Estimates per section for CT scans obtained at 125 kV(p).

angulation of the section plane is usually in the direction opposite that used in this study. In our experience, this angulation usually does not exceed 15° from the optimal perpendicular plane. Therefore, errors in perception of anatomic relationships are negligible.

Although our study showed a statistically significant interobserver variability, reanalysis of the data using the scores from the four neuroradiologists showed an improved correlation ($P > .05$). Despite a priori consenus, the interobserver variability may have been due in part to differences in approach and interpretion of complex, detailed scans. Moreover, the neuroradiologists in the study all trained and work at the same institution, thus potentially dampening individual variation in image analysis.

Finally, despite the limited number of cadaveric heads scanned (n = 2), we found a significant difference in the definition of the 10 anatomic landmarks between the two subjects, even after controlling for protocol and subject variability. This emphasizes the high prevalence of normal anatomic variability in the sinonasal complex that can influence image interpretation, contribute to the pathophysiology of inflammatory sinus disease, and add to the difficulty of performing functional endoscopic sinus surgery (14).

In conclusion, we propose an optimal scanning protocol for the examination of the paranasal sinuses using a direct coronal plane with a scanning angle not exceeding 10° from the plane perpendicular to the hard palate, 3-mm-thick contiguous sections, exposure factors of kV(p) = 120, mA = 80, detail reconstruction algorithm, and intermediate window settings (window = +1700 HU, level = −300 HU). This protocol will provide excellent anatomic definition and orientation of the paranasal sinuses while significantly decreasing the radiation dose equivalent to patients.

References

1. Moss A, Parsons V. *Current Estimates from the National Health Interview Survey, United States: 1985*. Hyattsville, Md: National Center for Health Statistics; 1986
2. Kennedy DW, Zinreich SJ, Rosenbaum AE, Johns ME. Functional endoscopic sinus surgery. *Arch Otolaryngol Head Neck Surg* 1985;111:576–582
3. Zinreich SJ, Kennedy DW, Rosenbaum AE, et al. Paranasal sinuses: CT imaging requirements for endoscopic surgery. *Radiology* 1987;163:769–775
4. Hilding AC. The physiology of drainage of nasal mucosa. *Ann Otolaryngol* 1944;53:35
5. Drettner B. The obstructed maxillary ostium. *Rhinology* 1967;51: 100–104
6. Messerklinger W. On drainage of the normal frontal sinus of man. *Acta Otolaryngol* 1967;673:176–181
7. Vinning EM, Kennedy DW. Surgical management in adults: chronic sinusitis. *Immunol Allerg Clin North Am* 1994;14:97–112
8. Hudgins P, Browning D, Gallups J. Endoscopic paranasal sinus surgery: radiographic evaluation of severe complications. *AJNR Am J Neuroradiol* 1992;13:1161–1167
9. White PS, Robinson JM, Stewart IA, et al. The CT mini-series: an alternative to standard paranasal sinus radiology. *Aust N Z J Surg* 1990;60:25–29
10. White PS, Cowan IA, Robertson MS. Limited CT scanning techniques in screening CT of the sinuses. *J Laryngol Otol* 1991;105: 20–23
11. Chow JM, Mafee MF. Radiologic assessment preoperative to endoscopic sinus surgery. *Otolaryngol Clin North Am* 1989;22:691–701
12. Babbel R, Harnsberger HR, Nelson B, et al. Optimization of techniques of the paranasal sinuses. *AJNR Am J Neuroradiol* 1991; 12:849–854
13. Duvoisin B, Landry M, Chapuis L, et al. Low-dose CT and inflammatory disease of the paranasal sinuses. *Neuroradiology* 1991; 33:403–406
14. Laine F, Smoker W. The ostiomeatal unit and endoscopic surgery: anatomy, variations, and imaging findings in inflammatory diseases. *AJR Am J Roentgenol* 1992;159:849–857